Highly Efficient Spectral Hole-Burning in Oxygen-Evolving Photosystem II Preparations †

ARTICLE *in* THE JOURNAL OF PHYSICAL CHEMISTRY B · JULY 2004

Impact Factor: 3.3 · DOI: 10.1021/jp0492523

6 AUTHORS, INCLUDING:

Elmars Krausz
Australian National University
218 PUBLICATIONS **3,335** CITATIONS
SEE PROFILE

Ron J Pace
Australian National University
95 PUBLICATIONS **3,391** CITATIONS
SEE PROFILE

Highly Efficient Spectral Hole-Burning in Oxygen-Evolving Photosystem II Preparations†

Joseph L. Hughes,‡ Barry J. Prince,‡ Elmars Krausz,*,‡ Paul J. Smith,§ Ron J. Pace,§ and Hans Riesen⊥

Research School of Chemistry, The Australian National University, Canberra ACT 0200, Australia, Faculties Chemistry, The Australian National University, Canberra ACT 0200, Australia, and School of Physical, Environmental and Mathematical Sciences, University College, The University of New South Wales, ADFA, Canberra ACT 2600, Australia

Received: February 18, 2004; In Final Form: May 14, 2004

We present the first report of highly efficient persistent spectral hole-burning in *active* (oxygen-evolving) Photosystem II (PSII) preparations. Samples are poised in the S_1 state of the Kok cycle, with the primary quinone (Q_A) either neutral or photoreduced to Q_A^- via a low-temperature pre-illumination. Remarkably efficient hole-burning is observed within the chlorophyll $Q_y(0,0)$ absorption envelope in the wavelength range of 676−695 nm. The hole-burning action spectrum of a sample poised in the $S_1(Q_A^-)$ state is dominated by a narrow feature (∼40 cm^{-1}) at 684 nm, where hole depths of 30% are attainable. The photoproduct for spectral holes burnt in this region is distributed across the ∼50 cm^{-1} absorption feature centered at 683.5 nm, independent of the excitation wavelength within this band. Saturated hole-burning experiments indicate weak electron−phonon coupling near 684 nm but stronger coupling for holes burnt near 690 nm. Selective excitation near 690 nm of samples in the $S_1(Q_A)$ state also results in efficient Q_A^- formation. Negligible hole-burning activity is observed at higher energies (<676 nm). Holewidths extrapolated to zero fluence and temperature are 2.0 ± 0.5 GHz near 685 nm for PSII samples in the $S_1(Q_A^-)$ state. Holewidths are twice as large and hole-burning quantum efficiencies are up to an order of magnitude greater (approaching 1%) for samples in the $S_1(Q_A)$ state. We ascribe hole-burning near 684 nm to slow (40−210 ps) excitation transfer from a CP43 chlorophyll to the PSII reaction center, and we ascribe hole-burning at ∼690 nm to excitation transfer from a chlorophyll in CP47. The unusually high hole-burning efficiency that we observe is attributed to a mechanism that involves charge separation in the reaction center that follows excitation transfer from these "slow transfer" states in CP43 and CP47. A key result of this work is the observation that selective excitation in the range 685−695 nm leads to efficient charge separation, as indicated by Q_A^- formation. This indicates the presence of (a relatively weak) P680 absorption in a native PSII, extending to low energy and underlying the CP47 chlorophyll trap absorption.

1. Introduction

1.1. Photosystem II and P680. Photosystem II (PSII) is a complex multiprotein transmembrane assembly found in all O_2-evolving photosynthetic organisms. The entire PSII assembly consists of a core complex, and a system of light-harvesting antenna proteins. A fully functioning PSII core complex consists of pigment-containing D1, D2, CP43, and CP47 proteins, and an integral cytochrome b_{559} (cytb_{559}) protein. The manganese catalytic site at which water oxidization occurs is bound to D1. Other smaller pigment-free peptides are involved in the stabilization of active PSII.[1] The D1/D2 heterodimer is analogous to the L and M proteins in the bacterial reaction center[2] and contains the redox-active pigments (Figure 1).

The availability of 3.4−3.8-Å resolution X-ray crystal structures[3−5] of membrane-bound PSII core complexes of thermophilic cyanobacteria has significantly aided spectroscopic studies of PSII. These relatively low-resolution X-ray structural data have confirmed the general arrangement of pigments and redox centers within a cyanobacterial PSII core. There is a significant homology of the major cyanobacterial and plant PSII core proteins,[2] as well as a strong similarity of cyanobacterial and plant PSII functions. This allows us to assume an analogous PSII organization in plants and cyanobacteria.

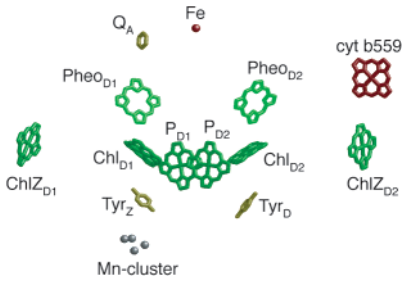

Figure 1. Arrangement of PSII reaction center chromophores taken from the crystal structure reported by Zouni et al.[4] The four central chlorophyll molecules are labeled P_{D1}, P_{D2}, Chl_{D1}, and Chl_{D2}. The peripheral chlorophyll molecules are labeled $ChlZ_{D1}$ and $ChlZ_{D2}$, whereas the D1/D2 pheophytin molecules are labeled $Pheo_{D1}$ and $Pheo_{D2}$, respectively. The quinone electron acceptor molecule (Q_A) and the non-heme Fe are indicated, along with the heme group of the cytb_{559} subunit, the redox active tyrosine protein residues Tyr_Z and Tyr_D, and the Mn-cluster.

† Part of the special issue "Gerald Small Festschrift".

* Author to whom correspondence should be addressed. Fax: +61-2-6125-0750. E-mail address: krausz@rsc.anu.edu.au.

‡ Research School of Chemistry.

§ Faculties Chemistry.

⊥ The University of New South Wales.

10.1021/jp0492523 CCC: $27.50
Published on Web 06/09/2004

The D1 and D2 protein subunits are each comprised of five transmembrane helices and, together, bind all the pigments of the reaction center. The D1 and D2 proteins each bind three chlorophyll *a* molecules (chl *a*) and one pheophytin *a* (pheo *a*). One chl *a* from each of the D1 and D2 proteins is bound to the periphery of the D1 and D2 proteins, and they are known as peripheral chl *a*, or ChlZ, leaving four central chl *a* and two pheo *a*. The plastoquinone electron acceptors, Q_A and Q_B, are bound to the D2 and D1 proteins, respectively. A non-heme Fe ion is located between these plastoquinones. Situated between the Mn-cluster and the four central chl *a* pigments are two redox-active tyrosine protein residues, D1-161 (Y_Z) and D2-160 (Y_D), as shown in Figure 1. There are two β-carotenes in the reaction center, and crystallographic evidence indicates that both β-carotenes are within the D2 protein.[3,5] The Mn-cluster is the site of catalytic water oxidization and lies at the luminal edge of the D1 protein.

The nature of the primary electron donor is currently being debated. We use the term P680 as a generic description of the photoactive assembly in PSII in either its native or isolated form. An excited state of P680 (P680*) is highly oxidizing and initiates the primary photochemistry of PSII. The degree of coupling between the four central chl *a* (see P_{D1}, P_{D2}, Chl_{D1}, and Chl_{D2} in Figure 1) and the two pheo *a* bound to the D1 and D2 proteins (see $Pheo_{D1}$ and $Pheo_{D2}$ in Figure 1) of PSII is under continued discussion.[6,7] Monomeric, dimeric, and multimeric models have been proposed for P680.[6,7]

The inner antenna proteins (CP43 and CP47) are intimately associated with the D1/D2/cytb_{559} proteins. The CP43 and CP47 pigment−proteins in spinach cores are estimated to contain 12 and 14 chl *a*, respectively.[1] In both CP43 and CP47, these chl *a* molecules are arranged in two layers, which are associated with the stromal and luminal regions of the proteins.[3−5] They serve as "inner" light-harvesting subunits and act as a conduit for excitation transfer from the main light-harvesting assembly to P680. The outer antenna light-harvesting assemblies of PSII are not directly involved in its redox chemistry; however, they do serve to transfer electronic excitation to P680 via CP43 and CP47.

Photoactivated electron flow only occurs through the D1 protein. Primary charge separation involves the rapid reduction of the $Pheo_{D1}$ by P680* to form $P680^+Pheo_{D1}^-$. Secondary electron transfer from $Pheo_{D1}^-$ to Q_A occurs within ~200 ps.[6,7] $P680^+$ oxidizes the redox active tyrosine, Y_Z, in nanoseconds,[6,7] which, in turn, oxidizes the Mn-cluster on a millisecond time scale.[6,7] There are four sequential one-electron light-driven oxidative steps of the Mn-cluster in PSII, which are described by the Kok cycle.[2] In this manner, the Mn-cluster is progressively advanced from the lowest oxidation state (S_0) to the S_1, S_2, S_3, and S_4 states. Oxygen is evolved at the catalytic Mn site in the S_4 state, returning the system to the S_0 state. The room-temperature, dark-adapted state of PSII is S_1.

A PSII preparation can be poised in a specific S state by appropriate illumination protocols and then trapped by rapid freezing. Detailed spectra of a range of metastable S-state species can thus be obtained. There have been numerous electron paramagnetic resonance (EPR) studies of the S_0-S_3 states at low temperatures (for recent reviews, see refs 8−11). If a PSII sample is illuminated at a temperature of <200 K, manganese oxidation is inhibited and alternative electron donors are utilized by the system.[12,13] Electrochromic shifts of nearby chromophores are associated with Q_A^- radical anion formation. These are conveniently studied via low-temperature (1.7 K) illumination of a sample poised in the S_1 state. The $S_1(Q_A^-)$ state is formed with a high quantum efficiency (≥0.1) and is stable over a period of hours.[14]

Spectral assignments of P680 remain the subject of ongoing discussion.[6,7] Significant spectral congestion is inherent in the optical spectra of PSII core complexes. This is partially due to the presence of chl *a* associated with both CP43 (12 chl *a*) and CP47 (14 chl *a*), whose absorption due to Q_y-state transitions is in the same spectral range as those due to the Q_y-state transitions of the D1/D2 chl *a* and pheo *a*. Another contributing factor is that weaker coupling exists, particularly between the P_{D1} and P_{D2} pigments, compared to their analogues in the bacterial reaction centers. This results in the energy separations of coupled chromophores being less than or equal to the spectral inhomogeneity in PSII cores.

To circumvent this spectral congestion, optical experiments that seek to probe the reaction-center pigments are commonly performed on D1/D2/cytb_{559} preparations. An added advantage of these preparations is that photochemistry beyond the primary charge separation step is inhibited by the absence of secondary electron donors and acceptors. Charge recombination of $P680^+Pheo_{D1}^-$ is rapid (40−100 ns, depending on temperature) (see Groot et al.[15] and references therein), allowing repeated measurement of charge-separation kinetics via transient absorption or time-resolved fluorescence, for example. In contrast, the illumination of a core complex leads to the efficient formation of relatively stable species. If measurements are made at room temperature, the sample can be continuously regenerated or replaced. However, low-temperature experiments are more difficult, as a range of photoproducts accumulate with a wide range of efficiencies. D1/D2/cytb_{559} preparations degrade with prolonged or intense illumination.[16]

We have suggested that the native D1/D2/cytb_{559} assembly becomes disrupted upon the detergent reduction of a core complex into protein components.[1,14,17,18] Relatively severe detergent treatment is required to remove CP43 and CP47, compared to the procedures used to make active cores. This may affect the conformation and homogeneities of the D1/D2 proteins. As a consequence, spectra of pigments in the D1/D2/cytb_{559} preparation do not fully reflect the properties of native P680 present in active PSII. In contrast, we have shown that spectral features—particularly, the prominent feature at 683.5 nm—are quantitatively retained in membrane-bound PSII and solublized PSII core complexes.[1,14] Absorption, circular dichroism (CD), magnetic circular dichroism (MCD), and electrochromism data were used to associate the prominent feature at 683.5 nm with P680.[19] We have established[17,20] that a CP43 absorption feature in this region cannot fully account for the 683.5 nm feature in PSII cores, unless the CP43 feature undergoes a 2-fold decrease in intensity upon isolation from the PSII core.

1.2. Charge and Excitation Transfer in the Photosystem II Reaction Center. Charge separation and subsequent photochemistry in PSII occurs by spontaneous ionization of the excited state of P680 (P680*). Numerous studies that use a range of approaches have attempted to determine rates of primary charge separation and excitation transfer processes in PSII, without a final consensus. There is much less spectral congestion and inhomogeneity in the spectra of bacterial reaction centers, compared to that of PSII. As a consequence, charge separation in the bacterial reaction center is better understood than the process in PSII.[2] There is significant structural and functional similarity between the two systems and results from studies on bacterial reaction centers have often served as a model for processes in PSII.[2,21] The rate for reduction of the bacteriopheo-

phytin in bacterial reaction centers, via charge separation of the primary donor near room temperature, is $\sim(3\ \text{ps})^{-1}$.[22] Excitation into any of the Q_y absorption bands in the reaction centers of purple bacteria at 10 K leads to excitation localization on the primary donor within 100 fs (see Durrant et al.[23] and references therein).

Despite the lack of agreement regarding the rates of energy and charge transfer in PSII, some aspects have gained a general consensus. Excitation transfer among the central D1/D2 chromophores (excluding the peripheral chl *a*) is generally accepted to be rapid and occurs on a sub-picosecond time scale.[7,22,24] Excitation transfer from the peripheral chl *a* (ChlZ) to the central four D1/D2 chromophores is thought to occur on a 10−50 ps time scale.[7,22,24] The majority of studies discussed in the review articles referenced[7,22,24] have reported work at or near room temperature. In native photosynthetic assemblies, the majority of P680* will form via excitation transfer from the inner antennae CP43 and CP47, following transfer from light-harvesting assemblies, rather than via the direct excitation of P680 itself.

1.3. Native Photosystem II. For the reasons outlined above (i.e., the accumulation of metastable species at low temperature), fast transient measurements on O_2-evolving PSII preparations have been made at room temperature. It has been argued that charge separation is more efficient when Q_A is oxidized (neutral).[25] The fluorescence efficiency increases markedly (by a factor of 3) when Q_A is maintained in the oxidized state by chemical treatment.[25] Kinetic measurements at room temperature of fluorescence and absorption changes in O_2-evolving PSII samples that contained ∼80 chl *a* per core complex showed processes with time constants of ∼80−120 ps for open PSII (Q_A oxidized) and ∼170−260 ps for closed PSII (Q_A reduced).[25] From these data, a model was developed[26] in which the intrinsic primary charge separation rate was determined to be $(2.7\ \text{ps})^{-1}$. The model explained the observed relatively slow kinetics by assuming fast (<2 ps) excitation equilibration among all the antenna chl *a* and the primary donor. In this trap-limited model, P680 acts as a shallow trap for excitation.

Schelvis et al.[27] have performed time-resolved picosecond absorption measurements at room temperature on O_2-evolving PSII core preparations with ∼35 chl *a* per core. The experiments were performed on closed PSII (Q_A reduced), and they observed kinetic components with time constants of 21, 80, and 200 ps. A wavelength dependence of the intermediate component (80−200 ps) was observed, whereas the 21 ps component was observed to dominate at longer wavelengths (∼690 nm). This wavelength dependence was used to argue *against* the possibility of fast equilibration of excitation between the entire antenna and P680. Transient experiments at 77 K on isolated CP43 and CP47[28] have identified a $(2-3\ \text{ps})^{-1}$ rate that connects pigments bound to the stromal and luminal sides of the membrane. It was suggested that energy transfer from CP43 and CP47 to the reaction center will occur from those chl *a* on the stromal side of these inner antennae. Again, the $(2-3\ \text{ps})^{-1}$ kinetic component is too slow to be easily consistent with the shallow trap model for PSII cores.

1.4. D1/D2/cytb_{559}. There is ongoing discussion regarding interpretation of results obtained from studies on D1/D2/cytb_{559} preparations. At low temperature, a primary charge separation rate of $\sim(1-3\ \text{ps})^{-1}$ is generally accepted, whereas at room temperature, rates from $(1-3\ \text{ps})^{-1}$ up to $\sim(20\ \text{ps})^{-1}$ are still debated.[7,22,24] At low temperatures, the fast kinetics directly observed are multiphasic, with components ranging from $(1-3\ \text{ps})^{-1}$ up to $(20-30\ \text{ps})^{-1}$ and $(100-200\ \text{ps})^{-1}$.[7,22,24] Fast transient experiments are prone to nonlinear effects and also sample degradation at the high powers, which are inherent in even the lowest fluence experiments.[16,29−31]

Two-pulse photon-echo experiments[32] were performed at 1.3 K with minimal pulse energies and were analyzed via a model to provide an intrinsic charge separation rate of $(1.5\ \text{ps})^{-1}$, although a wide range of kinetics was invoked. More direct recent experiments[33] made at 77 K on several D1/D2/cytb_{559} preparations have indicated a $(3.1\ \text{ps})^{-1}$ rate in the usually studied preparation and a $(0.8\ \text{ps})^{-1}$ rate in a sample where $Pheo_{D2}$ was replaced by a chemically modified pheophytin.

Hole-burning spectroscopy[34,35] is a frequency-domain experiment in which the holewidth can provide information on the lifetime of the excited state(s) of the chromophores involved. A homogeneous holewidth of 1 GHz corresponds to an excited-state lifetime of 318 ps. Such experiments can be performed at very low fluence and provide a useful adjunct to fast pump−probe spectroscopies. Persistent spectral hole-burning has been performed on D1/D2/cytb_{559}, providing information on strongly fluorescent trap pigments with lifetimes of ∼4 ns, which are present in these samples but are not involved in charge separation.[15,36] We are aware of only one report of primary donor pigments in any photosynthetic reaction centers displaying persistent spectral hole-burning.[37] These experiments were performed at a very high fluence (225 J/cm^2). Transient hole-burning is possible in D1/D2/cytb_{559} via the formation of a long-lived (millisecond time scale) ^{3}P680 state, which follows charge recombination of $P680^+Pheo_{D1}^-$. The most recent report of transient ^{3}P680 hole-burning[38] provides a holewidth that is compatible with a charge-separation rate of $(4.6\ \text{ps})^{-1}$.

1.5. Hole-Burning in Oxygen-Evolving Photosystem II. In this paper, we investigate the high-efficiency persistent spectral hole-burning in active, O_2-evolving PSII preparations. To our knowledge, there has been only one report[39] of persistent spectral hole-burning in active PSII. These experiments were performed at a very high laser fluence, leading to shallow and broad spectral holes. We are not able to reproduce their results. The current study was undertaken to provide information on the spectral position, excited-state lifetimes, and electron−phonon coupling of longer-lived excitations within PSII cores.

2. Materials and Methods

Membrane-bound PSII-enriched material (BBY) was isolated from spinach, as previously described.[1] PSII core complexes containing ∼32 chl *a* per core were prepared from membrane-bound PSII, also as previously described.[1] These PSII cores have comparable O_2-evolving activity to the membrane-bound preparation. *Synechocystis* 6803 (*syn*. 6803) cyanobacterial PSII core complexes were prepared as described in Peterson Årsköld et al.[14] These concentrated preparations (1−5 (mg chl *a*)/mL) were stored in the dark in sucrose buffers at 77 K. For spectroscopic measurements, samples were rapidly thawed then diluted in the elution buffer and mixed with an ethylene glycol/glycerol (1:1) glassing medium to a final concentration of 40%−50%, achieving a maximal optical density of ∼1 in the chl *a* Q_y spectral region. All sample handling was performed under dim green light. The prepared sample cell was left in darkness for 5 min at room temperature before rapid freezing to the data collection temperature (1.7 K). Spectral holes were measured in transmission.

For absorption spectra and broadband hole-burning measurements, a 12-mm-diameter quartz-windowed cell assembly with a path length of 150 μm was utilized. An Oxford Instruments Spectromag 4 cryostat was used. Glasses of high optical quality

were obtained by lowering the cell, fixed to the sample rod, into liquid helium. Cooling from 300 K to 4 K occurred over a time period of ~30 s. The liquid helium was then pumped to perform transmission experiments in bubble-free superfluid helium. Absorption features $<10^{-4}$ could be reliably measured.

The spectrometer used for absorption and broadband hole-burning measurements was designed and constructed in our laboratory and has been described in detail elsewhere.[1,40] The spectra presented in this report were recorded with 50-mm slit widths (0.03 nm resolution) using a Hamamatsu R669 photomultiplier tube for detection. The measurement beam was expanded to approximately the diameter of the sample cell (12 mm), to minimize actinic effects of the measurement light.

Broadband spectral holes were burnt with a Spectra-Physics model 375 dye laser that was operating with DCM dye and pumped by a Spectra-Physics model 171 Ar* ion laser. Wavelength selection of the dye laser was achieved using a two-plate birefringent filter so that the width of spectral holes was purposely expanded to $2-3$ cm^{-1} by the line width of the laser. This matches the resolution of the spectrometer and avoids artifacts due to a sharp, unresolved hole-burning feature.

For the high-resolution spectral hole-burning measurements, the prepared sample (as above) was placed into a 1.5-mm-path-length sapphire-windowed cell and mounted on the coldfinger of a closed-cycle refrigerator (Janis/Sumitomo SHI-4.5). The sample cooling time to ~2.5 K was ~2 h. The mounted sample was cooled to -50 °C in <30 min and was at a temperature of >270 K for <10 min. A Lakeshore model 330 auto-tuning temperature controller was used to monitor a silicon diode thermometer mounted on the coldfinger of the closed-cycle refrigerator. The sample temperature was calibrated by measuring the fluorescence emission of the R-lines of a NaMgAl(oxalate)$_3$·9H$_2$O:Cr(III) crystal, as a function of temperature.[41] The relative amplitudes of the Cr(III) R_1- and R_2-line emission are accounted for by a Boltzmann population. Hole-burning was achieved, and transmission spectra recorded, using an Hitachi model HL6738MG laser diode mounted on a Thorlabs model TCLDM9 thermoelectric mount. The current and temperature of the 690-nm laser diode were maintained and controlled by Thorlabs model LDC500 and TEC2000 current and temperature controllers, respectively.[41,42] A schematic diagram of the high-resolution hole-burning apparatus is presented in Figure 2.

The frequency of single-mode laser diodes can be tuned by varying the injection current. The frequency/current tuning ratio of the diodes used in this work was on the order of -2.5 GHz/mA. The current controller (Thorlabs model LDC500) allows for the external modulation of the injection current, for which we used a 2000 or 2500 Hz triangular waveform provided by a Stanford model SRS DS345 function generator. Mode-hop free scans of $\sim 30-40$ GHz were possible for the diodes used in the experiments reported here. A diode voltage amplitude change of ± 10 mV corresponded to a current modulation of ± 0.5 mA and, thus, a frequency scan of approximately ∓ 1.25 GHz. A Coherent model 240 spectrum analyzer, with a free spectral range of 300 MHz, was used to calibrate the wavelength scan.

Hole readout in transmission was achieved using a silicon photodiode (Thorlabs model PDA55-EC), or a Hamamatsu 3-mm model S2384 silicon avalanche photodiode. These detectors had high quantum efficiency ($>70\%$) at 690 nm and, for this reason, were used in preference to photomultipliers. Care was taken to focus a large fraction of the transmitted laser light on the detector, to allow the highest possible sensitivity of hole-readout for a given light fluence. The transmission signal was

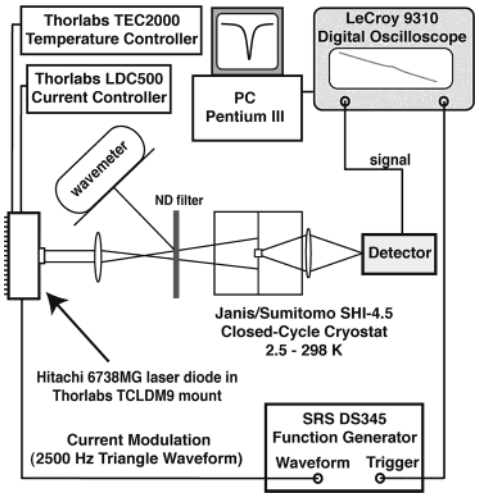

Figure 2. Schematic diagram of the experimental diode-laser hole-burning apparatus. The diode-laser has a line width of ~20 MHz and is tuned by varying the injection current. The injection current is modulated by a triangular waveform, typically with a frequency of 2500 Hz, which is provided by a function generator. The laser light is defocused onto the sample to a beam size of ~0.6 cm^2. All the light transmitted through the sample is focused onto the detector, and the data are accumulated on an 11-bit digital oscilloscope and then subsequently transferred to a personal computer. (See Materials and Methods for further information.)

accumulated and averaged on either an 8-bit (*y*-resolution) Tektronix model TDS210 or an 11-bit (*y*-resolution) LeCroy model 9310 digital oscilloscope and, subsequently, on a Pentium-III-based personal computer. Under the operating conditions used, the laser line width was 20 MHz.

For hole-burning, the laser was kept at constant current and, thus, constant wavelength, and the light was attenuated by an initial neutral density (ND) filter, before being defocused at the sample to a beam size of ~0.6 cm^2. The reflected beam from the ND filter was monitored by a wavemeter to determine the excitation wavelength. Additional ND filters were then placed between the laser and the cryostat, to achieve the desired laser intensity for hole-burning. For hole readout, the beam was further attenuated by additional ND filters to a point where minimal additional hole-burning occurred.

3. Results

3.1. Low-Temperature Q_A^- Formation. Figure 3 shows the 1.7 K absorption spectrum in the $Q_y(0,0)$ region of a spinach PSII core complex after dark adaptation and before any illumination, with PSII poised in the $S_1(Q_A)$ state. The spectrum is well-structured, with a prominent sharp (~50 cm^{-1}) feature at 683.5 nm whose area corresponds to ~2 chl *a*.[1] Illumination of the sample at low temperature leads to measurable changes in the $Q_y(0,0)$ region. These are paralleled by much-larger relative changes of the absorption in the region near 540 nm associated with the Q_x transition of pheo *a*.[14] The difference of the absorption spectra collected before and after continuous wave (CW) illumination at 1.7 K reveals changes in transitions that occur due to the illumination. Figure 3 shows a series of difference spectra taken at 1.7 K with illumination at 630 nm. The fluences used to obtain the difference spectra of Figure 3 span 3 orders of magnitude, ranging from 16 μW/cm^2 for 10 s (160 μJ/cm^2) to 4.9 mW/cm^2 for 33 s (162 mJ/cm^2).

An analysis[14] of difference spectra obtained after high- (270 K) and low-temperature (1.7 K) illumination of PSII core complexes has assigned the prominent derivative feature

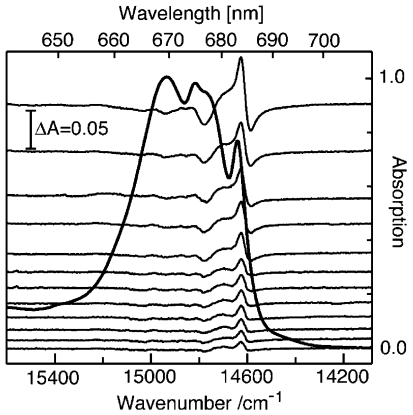

Figure 3. Absorption spectra (thick line) at 1.7 K of a spinach PSII core complex, in the $S_1(Q_A)$ state before illumination, and absorption difference spectra (thin lines) after illumination of a PSII core in the $S_1(Q_A)$ state, showing the electrochromic shift in the $Q_y(0,0)$ region that occurs due to illumination-induced Q_A^- formation. All illuminations were conducted at 630 nm and 1.7 K. The illumination fluences producing these difference-spectra ranged from 160 μJ/cm^2 (bottom) to 162 mJ/cm^2 (top).

centered near 685 nm in spinach and 683 nm in cyanobacterial PSII as an electrochromic shift of the $Q_y(0,0)$ transition of $Pheo_{D1}$. This electrochromic shift is associated with the formation of Q_A^-. In low-temperature illuminations, the secondary electron donor was identified as the heme Fe(II) of cytb_{559} in BBY samples, and a β-carotene in core complexes. Under physiological conditions, the Mn-cluster reduces $P680^+$ in both preparations. It was established[14] that the secondary electron donors have a minimal effect on the difference spectra, such as those in Figure 3, and that the 683.5 nm feature is also minimally affected.

The series of spectra in Figure 3 establish that the illumination-induced changes do not lead to significant chl *a* radical formation. Any such radical formation would lead to the difference spectra displaying a net decrease in absorption (not conservative) in the chl *a* region. We find that the absorption differences are conservative to within 0.05 chl *a* per PSII core complex. Although initial Q_A^- formation is more efficient for lower fluences, the shapes of all illumination-induced difference spectra are independent of illumination fluence and wavelength in the 500−700 nm range. At much-higher fluences (>10 J/cm^2), sample damage can occur. The overall quantum efficiency of low fluence (<20 mJ/cm^2) and low-temperature Q_A^- formation has been estimated as ∼10%,[14] which is in agreement with the data in Figure 3.

3.2. Broadband Spectral Hole-Burning. Figure 4 shows the effects of broadband (2−3 cm^{-1} width) laser excitation of a PSII spinach core complex poised in the $S_1(Q_A)$ state and also in the photoreduced $S_1(Q_A^-)$ state. The hole-burned spectra are the differences of the absorption spectra in the $Q_y(0,0)$ region before and after laser illumination. Persistent spectral hole-burning was conducted with a laser power of ∼3.5 mW/cm^2 for 60 s at 683.3 nm for the spectra in Figure 4. The hole-burned spectrum of a sample poised in the $S_1(Q_A)$ state displays a spectral hole superimposed upon a background with considerable structure. This structured background is due to the Q_A^- shift, as seen in Figure 3. No persistent spectral hole-burning was observed with laser wavelengths of <675 nm. However, as mentioned previously, efficient Q_A^- formation occurs for excitation at higher energies.

To perform measurements on PSII in the $S_1(Q_A^-)$ state, a sample in the $S_1(Q_A)$ state was illuminated with laser light at

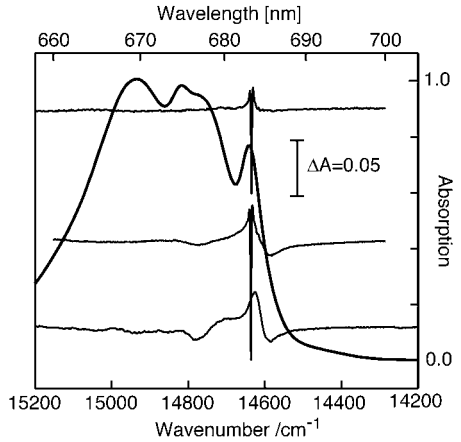

Figure 4. Absorption spectra (thick line) at 1.7 K of a spinach PSII core sample prepared in the $S_1(Q_A)$ state before illumination. Broadband (laser line width of ∼2−3 cm^{-1}) hole-burned spectra of a spinach PSII core in the $S_1(Q_A^-)$ state (top) and $S_1(Q_A)$ state (center) at 1.7 K. Hole depths (($\Delta A/A$) × 100%) are ∼9% and ∼12%, respectively, each attained with ∼3.5 mW/cm^2 for 60 s. The bottom trace shows Q_A^- formation, following 630-nm illumination with comparable burn fluence to the hole-burned spectra. Hole-burning with PSII in the $S_1(Q_A)$ state results in a persistent spectral hole superimposed on the structure associated with electrochromic shifts due to Q_A^- formation. With PSII in the $S_1(Q_A^-)$ state, difference spectra after laser illumination at ∼683 nm display persistent spectral hole-burning features only, because all PSII centers have been converted to the $S_1(Q_A^-)$ state.

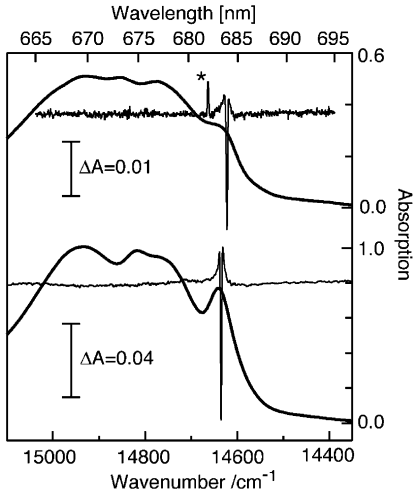

Figure 5. Absorption spectra of *syn.* 6803 (top, thick line), and spinach (bottom, thick line) PSII core complexes in the $S_1(Q_A)$ state at 1.7 K. Hole-burned spectra show persistent spectral holes burnt with a broadband laser (line width of 2−3 cm^{-1}) in *syn.* 6803 (top, thin line) and spinach (bottom, thin line) PSII cores at 1.7 K. Hole depths are ∼7.5% (top, thin line) and ∼10% (bottom, thin line), burnt with ∼1.4 mW/cm^2 for 10 s, and ∼3.5 mW/cm^2 for 60 s, respectively. The asterisk (*) indicates laser-induced hole-filling of a previously burnt hole.

630 nm with a similar fluence to that used for hole-burning (above). Subsequent illumination at 683.3 nm results in a spectral hole, resonant with the laser frequency. This is formed with no background changes associated with Q_A^- formation as the 630 nm pre-illumination converts the sample quantitatively to the $S_1(Q_A^-)$ state. The photoproduct associated with hole formation is found on both sides of the resonant hole, and its distribution reflects that of the absorption feature at 683.5 nm.

Figure 5 compares broadband hole-burning of spinach and *syn.* 6803 core complexes poised in the $S_1(Q_A^-)$ state, both having been pre-illuminated at 630 nm. The hole depths (($\Delta A/A$) × 100%) are ∼10% and ∼7.5%, respectively. The sharp side-feature in the spectrum of *syn.* 6803, indicated by the

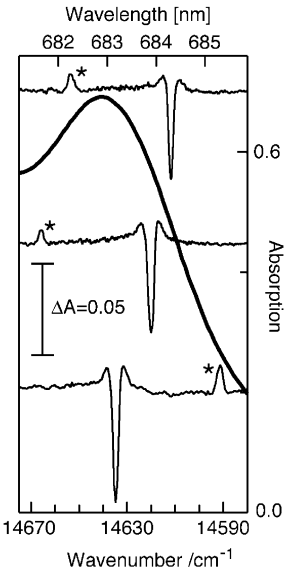

Figure 6. Absorption spectra (thick line) at 1.7 K of a spinach PSII core complex, in the $S_1(Q_A)$ state before illumination. Hole-burned spectra (thin lines) show the photoproduct distribution of persistent spectral holes burnt (broadband laser line width of 2−3 cm^{-1}) in a spinach PSII core in the $S_1(Q_A^-)$ state at 1.7 K, with ∼3.5 mW/cm^2 for 20 s. All hole depths are ∼9%−10%. This sharp photoproduct is superimposed on a broader underlying distribution, which is indicated by the shaded regions.

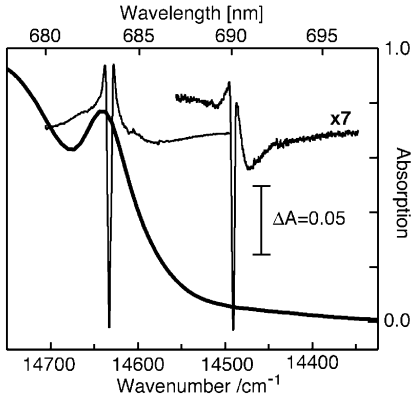

Figure 7. Absorption spectra (thick line) at 1.7 K of a spinach PSII core complex, in the $S_1(Q_A)$ state before illumination. Saturated hole-burned spectra show the different phonon structure (sidehole to lower-energy of 690.1 nm hole) of holes burnt with a broadband laser (line width of 2−3 cm^{-1}) at 683.4 and 690.1 nm in a spinach PSII core in the $S_1(Q_A^-)$ state at 1.7 K. The 690.1 nm hole (right) has been multiplied by a factor of 7 (×7). The hole depths are ∼17% (left) and ∼38% (right), attained with burn fluence of ∼15 mW/cm^2 for 5 min.

asterisk in Figure 5, is due to laser-induced hole-filling of a previously burnt hole. In both systems, photoproduct is distributed adjacent to the resonant spectral hole, to higher and lower energies. Figure 6 reveals closer details of the hole structure for a spinach core in the $S_1(Q_A^-)$ state, indicating a broad photoproduct accompanied by a sharper photoproduct. There is no obvious preference for the sharp photoproduct to be either red- or blue-shifted. A detailed study of this narrow distribution photoproduct requires hole-burning with a narrow-band laser and readout at high resolution over a relatively large frequency range. We are not currently able to perform such measurements.

In either plant or cyanobacterial PSII, there is no indication of sidehole structure outside the photoproduct region (see Figure 5). This result is in contrast to comparable hole-burning experiments performed on isolated CP43,[20,43] CP47,[44] and D1/D2/cytb_{559}[45,46] preparations. In these systems, significant changes occur across the entire $Q_y(0,0)$ spectral region.

No vibrational sideholes are observable in the 600−650 nm $Q_y(1,0)$ spectral region upon deep, saturated hole-burning near 684 nm. In contrast, we have previously been able to observe vibrational sidehole features in saturated hole-burning experiments on isolated CP43.[20] Laser excitation into the $Q_y(1,0)$ region of CP43 leads to deep sideholes in the $Q_y(0,0)$ origin.[20] No such sideholes were measurable in PSII cores complexes. This may be due to the larger number of chl *a* molecules in the core. Absorption spectra clearly show $Q_y(1,0)$ vibrational sideline structure associated with the 683.5 feature,[17] with line widths comparable to that of its $Q_y(0,0)$ origin. The complete absence of vibrational sideholes and the inability to observe hole-burning via excitation into vibrational sidelines in PSII cores highlights differences between intact cores and fragment proteins. Vibrational relaxation in $Q_y(1,0)$ in cores may be significantly faster than normally seen in chl *a* (1−3 ps)[47] or in isolated CP43,[20] leading to broader vibrational holes and sideholes. Because significant photoproduct is distributed close to the resonant hole, any broadening of a spectral hole will lead to the hole overlapping with photoproduct and a consequent decrease in the maximal depth of the hole. However, there is currently no physical model that would predict a shortening of vibrational relaxation time.

Excitation at a vibrational sideline wavelength of the 683.5 nm feature also excites other chl *a* pigments with vibrational sidelines absorbing at the same energy. Energy is then transferred to CP43 and CP47 chl *a* trap states. This results in hole-filling because the initial process that dominates the usual hole burning process via excitation transfer from vibrational excited states of a chromophore is now nonselective.

The saturated hole-burned spectra in Figure 7 reveal distinctly different phonon sidehole structure of holes burnt at 683.4 and 690.1 nm for a spinach PSII core in the $S_1(Q_A^-)$ state. The sidehole to the red side of the resonant hole at 690.1 nm is a pseudo-phonon sideband hole.[35,48] There is a significant reduction of the pseudo-phonon sideband hole associated with the resonant hole at 683.4 nm, compared to that observed at 690.1 nm. More-detailed studies are required to establish a quantitative comparison of electron−phonon couplings.

3.3. Hole-Burning Action Spectra. The hole-burning action spectra of BBY and core complex samples prepared from spinach, as well as for *syn*. 6803 core complexes, are shown in Figure 8. These action spectra were obtained with PSII in the $S_1(Q_A^-)$ state and monitor hole-burning as a function of wavelength using a constant laser fluence. The fluence was chosen to provide holes across the absorption envelope that are not deeply saturated. One of the first applications of this approach was to *R. sphaeroides*,[49] in which the site distribution function (SDF) of the lowest exciton component of the LH1 antenna complex was obtained.

The overall characteristics of the action spectra are similar for all our PSII preparations. Laser illumination at wavelengths of <670 nm was almost completely ineffective in hole formation. There is a narrow SDF centered at ∼684 nm that dominates the action spectra. From simple Gaussian fits, the prominent feature in the spinach core action spectrum is located at 683.8 nm with a width (fwhm) of 40 cm^{-1}, whereas that of *syn*. 6803 is centered at 683.6 nm with a width of 75 cm^{-1}. This difference may be attributed to differing inhomogeneous spectral distributions of the chromophore(s) that results in hole-burning in this region.

There are chromophores to both higher and lower energy of the narrow SDF that contribute to the action spectrum, extending

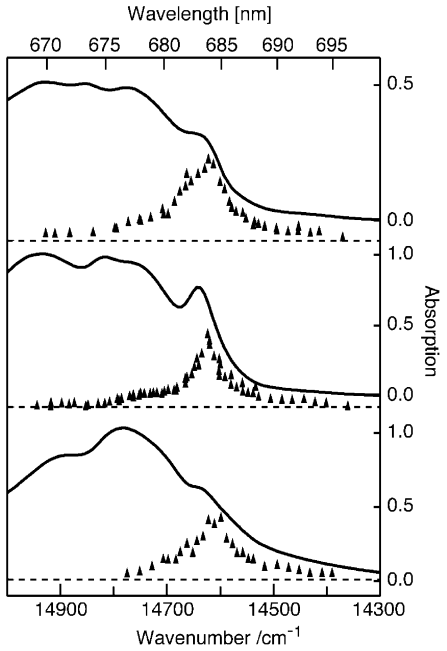

Figure 8. Absorption spectra (thick lines) at 1.7 K of *syn*. 6803 (top) and spinach (center) PSII cores, as well as spinach BBY (bottom) membrane-bound preparations. The triangles represent the hole-burning action spectra obtained by burning with constant fluence, and the solid curve represents the resultant hole area as a function of burn frequency. The horizontal dotted lines indicate the zero of the action spectrum, which are plotted on arbitrary *y*-axis scales. Hole-burning for the action spectra was performed at 1.7 K with broadband laser excitation (line width of 2−3 cm^{-1}), and with fluence such that holes were not deeply saturated ($(\Delta A/A) < 10\%$).

from 675 nm to 695 nm. The higher-energy component corresponds to hole-burning by a small fraction of the chromophores absorbing in the $Q_y(0,0)$ region. However, at wavelengths of <686 nm, where overall absorption is relatively weak, hole-burning is highly efficient, and hole depths of ∼50% can be achieved.

Spectral holes can be filled either by warming the sample to >30 K or by illumination of the sample at wavelengths of <670 nm. Systematic measurements with PSII in the $S_1(Q_A)$ state are more difficult than those for the $S_1(Q_A^-)$ state, because the laser illumination used in hole-burning leads to efficient Q_A^- formation. This results in the electrochromic shifts as seen in Figures 3 and 4, obscuring features that were solely due to hole-burning. In addition, it is not feasible to regenerate the $S_1(Q_A)$ state of a PSII sample quantitatively. Warming the sample to >150 K only partially regenerates the sample. Annealing the sample to 270 K does lead to full Q_A^- oxidization; however, when a sample is subsequently re-glassed, there can be subtle changes that make accurate comparisons of spectra previously obtained difficult.

By performing hole-burning measurements as a function of laser fluence, while also monitoring Q_A^- formation via broadband spectral changes (as in Figure 3), we were able to make estimates of hole-burning efficiencies for spinach PSII core complexes in both the $S_1(Q_A)$ and $S_1(Q_A^-)$ states over a range of wavelengths. Quantum efficiencies of persistent spectral hole-burning were as high as 10^{-2} with PSII in the $S_1(Q_A)$ state and 10^{-3} in the $S_1(Q_A^-)$ state. Laser burn fluences used in this work were as low as 50 nJ/cm^2 and, for high-resolution measurements, typically on the order of 1−10 μJ/cm^2. This is orders of magnitude lower than the fluences commonly used in hole-burning[50,51] and in two recently reported crystalline chromium systems that display initial nonphotochemical hole-burning quantum efficiencies of $\sim 10^{-3}-10^{-2}$.[52,53] Our hole-burning fluences are comparable to, and typically lower than, those used in amorphous systems that display the most-efficient nonphotochemical hole-burning.[54,55] Burn fluences utilized in hole-burning on photosynthetic antenna systems are also orders of magnitude higher than those used in this work (see, for example, hole-burning in the Fenna−Matthews−Olsen Antenna complex[56]). A spectral hole with a depth of 1.6% could be obtained near 684 nm in the $Q_y(0,0)$ absorption spectrum of a spinach PSII core in the $S_1(Q_A)$ state with defocused light from a 0.75 m monochromator/tungsten lamp system operating with 50-μm slit widths for 7 min. This corresponds to a fluence of ∼400 nJ/cm^2.

Hole-burning in PSII samples in the $S_1(Q_A)$ state is invariably accompanied by Q_A^- formation, as determined by broadband difference-spectra (as in Figure 1). These processes seem to have very comparable efficiencies. Q_A^- formation was observed following excitation in the 683-nm region but also following excitation in the 685−695 nm range. Prolonged low-intensity (<1 mW/cm^2) illumination in the range of 685−695 nm leads to full (approaching 100%) and efficient Q_A^- formation, accompanied by relatively deep spectral holes. In a control experiment, relatively intense excitation (100 mW/cm^2 for 10 min) at 750 nm led to no observable Q_A^- formation.

Q_A^- formation can only occur as a direct consequence of charge separation in P680*. Therefore, we are left with the surprising observation that either P680 absorbs directly in the 685−695 nm range or is excited by excitation transfer from other pigments that are also absorbing in this range. The remarkably high efficiency of hole-burning, particularly in the $S_1(Q_A)$ state, suggests that the hole-burning mechanism is associated with P680 excitation and subsequent charge separation. Absorption in this region has been associated with a well-known trap pigment in CP47 with a broad band whose maximum is near 690 nm.[57] The lowest-energy states of CP43 are relatively sharp and absorb near 683 nm.[43] These observations are given further consideration in the discussion section.

3.4. High-Resolution Spectral Hole-Burning. The previously described broadband experiments were performed with a dye laser operating at a relatively broad line width of 1−3 cm^{-1}. This allowed spectral changes over a very large wavelength range (440−750 nm) to be monitored with high sensitivity, using a conventional spectrometer operating with a spectral resolution comparable to the laser line width. To measure homogeneous holewidths, experiments with the much-higher resolution of ∼20 MHz (∼0.001 cm^{-1}) were performed using the diode−laser system described in the Materials and Methods section. Following hole-burning at a specific wavelength, the laser was attenuated and repeatedly scanned over ∼30 GHz (1 cm^{-1}). Spectral holes were measured in transmission, which is an approach that allows much-lower readout fluences than necessitated in fluorescence excitation experiments.

Measurements were performed on PSII spinach cores in the $S_1(Q_A^-)$ state by pre-illumination of dark-adapted samples using 632.8 nm radiation with ∼2 mW/cm^2 for ∼5 min. Hole-burning on PSII cores in the $S_1(Q_A)$ state was performed on samples annealed in the dark at 260−270 K for 5 min. Care was taken to ensure that the sample was kept dark before exposure to the laser at the burn wavelength, ensuring that contamination of the sample by PSII in the $S_1(Q_A^-)$ state was insignificant. All hole profiles were well-described as a single Lorentzian. The delay between burn completion and hole readout was typically

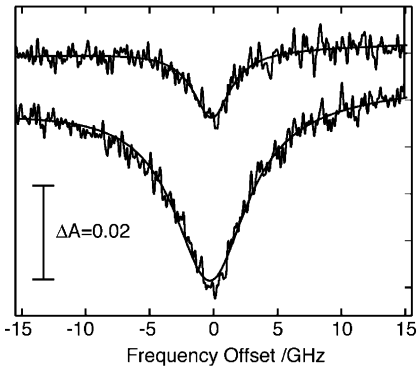

Figure 9. Typical persistent spectral holes burnt with a narrow band laser (line width of ~20 MHz) at 685.20 nm in a spinach PSII core in the $S_1(Q_A^-)$ state (top) and $S_1(Q_A)$ state (bottom) at 2.5 K. The burn fluence used for these holes was 67 nW/cm^2 for 60 s in each case, and the hole depths are 1.5% and 4.7%. The holes are well-described by Lorentzian line shapes, shown by the smooth curves overlayed on each trace, yielding line widths of 3.6 ± 0.1 GHz and 7.0 ± 0.3 GHz.

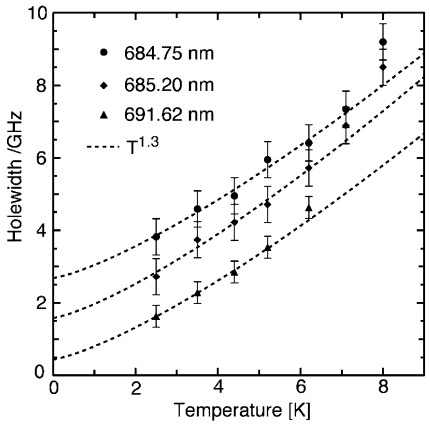

Figure 10. Temperature dependence of the holewidth of persistent spectral holes burnt at three different wavelengths with a narrow band laser (line width ~20 MHz) in spinach PSII core complexes in the $S_1(Q_A^-)$ state. Holewidths at each temperature have been extrapolated to zero burn fluence. Dotted lines show fits of $y = y_o + aT^{1.3}$, for $T < 6$ K.

<30 s and not greater than ~2 min. The hole depth can decay slightly (~15%) over a time period of ~2 min but negligible hole-broadening occurred during this time.

3.5. Hole-Burning Widths in $S_1(Q_A)$ and $S_1(Q_A^-)$. Figure 9 shows shallow persistent spectral holes burnt at 685.20 nm in the $Q_y(0,0)$ band in a spinach core sample in the $S_1(Q_A)$ (bottom) or $S_1(Q_A^-)$ (top) states. The hole depths are 4.7% and 1.5%, respectively. This burn wavelength is similar to the maximum of the hole-burning action spectrum in Figure 8. The fluence used for these holes was 67 nW/cm^2 for 60 s (4 mJ/cm^2). The signal-to-noise ratio of hole readout could be improved by extended averaging but was limited to ~50 scans to minimize the effect of temporal hole decay and laser-induced hole-filling. The contribution to the measured holewidth due to spectral diffusion was evaluated by varying the delay period between burn completion and hole readout from a few seconds to a few minutes. On the time scale of ~2 min for hole readout, spectral diffusion was small and within the holewidth variation of 0.5 GHz.

Figure 9 immediately indicates that hole-burning was ~5 times more efficient in the $S_1(Q_A)$ state, compared to the $S_1(Q_A^-)$ state. The holewidth was ~2 times broader, at 7.0 ± 0.3 GHz, compared to 3.6 ± 0.1 GHz in the $S_1(Q_A^-)$ state. The hole-burning efficiencies observed with the diode−laser system were fully consistent with parallel experiments performed via broad-band laser hole-burning and monochromator readout. Quantitative determinations of hole-burning efficiencies are made in a following section.

3.6. Excited-State Lifetimes. The dephasing processes associated with an electronic excitation determine the homogeneous line width of the zero-phonon line of an optical transition in the condensed phase. The dephasing time (T_2) has contributions from the excited-state lifetime (T_1) and a "pure dephasing" time (T_2*).[34,50] The pure dephasing process results from fluctuations of a single-site transition frequency induced by time-dependent interactions of the chromophore with its environment. The homogeneous line width (Γ_{hom}) is given by

$$\Gamma_{hom} = (\pi T_2)^{-1} = (2\pi T_1)^{-1} + (\pi T_2^*)^{-1}$$

In a hole-burning experiment where the laser line width is much less than the measured holewidth, this holewidth is twice the homogeneous line width ($\Gamma_{hol} = 2\Gamma_{hom}$). This is due to hole-burning involving at least two photons: one to burn and another to read the hole.[50,51] The lifetime-limited holewidth, $\Gamma_{hol} = (\pi T_1)^{-1}$, can be determined by extrapolating the measured holewidth to zero burn-fluence and zero temperature,[15,50,58] assuming the holewidth contribution due to T_2* vanishes. This process yields the lifetime-limited homogeneous line width and, consequently, a measure of the excited-state lifetime for the hole-burned chromophore.

The contribution from pure dephasing to the holewidth in spinach cores was determined by measuring the holewidth, extrapolated to zero fluence, at three wavelengths over the temperature range 2.5−10 K (Figure 10). The zero-fluence holewidths in the temperature range of 2.5−6 K can be fitted to the $T^{1.3}$ temperature dependence commonly used for chromophores in amorphous hosts[34,50] and the extrapolation to 0 K thus determined. The lifetime-limited holewidths obtained by a fit of $T^{1.3}$ dependence were 2.0 ± 0.5 GHz at 684.75 nm, 1.5 ± 0.5 GHz at 685.20 nm, and 0.5 ± 0.3 GHz at 691.62 nm. The corresponding excited-state lifetime estimates are 160, 210, and 640 ps, respectively.

Boxer et al.[59] provided the first report of nonphotochemical hole-burning in a well-defined protein matrix, along with the temperature dependence of the holewidth in the temperature range of 1.35−2.5 K. The hole readout was conducted in fluorescence excitation, and the width followed a $T^{1.3}$ temperature dependence. A $T^{1.3}$ temperature dependence has also been ascribed to the homogeneous holewidth in non-O_2-evolving PSII reaction centers isolated from spinach via fluorescence-detected hole-burning experiments.[15,36] In these latter experiments, the T_1 lifetime of chromophores absorbing maximally near ~681 nm was 4 ± 1 ns, which approaches the chl *a* radiative lifetime of 8 ns. A $T^{1.3}$ temperature dependence has also been reported[56] for the Fenna−Mathews−Olsen antenna complex. Hole-burning efficiencies in all the aforementioned reports seem to be much lower than those observed in this work, and, consequently, higher burn fluences (>100 mJ/cm^2) were necessary.

3.7. Hole-Growth Kinetics and Hole-Burning Quantum Efficiency. The initial hole-burning quantum efficiency (ϕ) can be estimated from the hole-growth kinetics. Typical kinetics for holes burnt with PSII in the $S_1(Q_A^-)$ state are shown in Figure 11. The dotted line through the data is provided as a visual aid only. The quantum efficiency is calculated from the ratio of the number of absorbing centers excited to the number of photons absorbed, while accounting for those chromophores

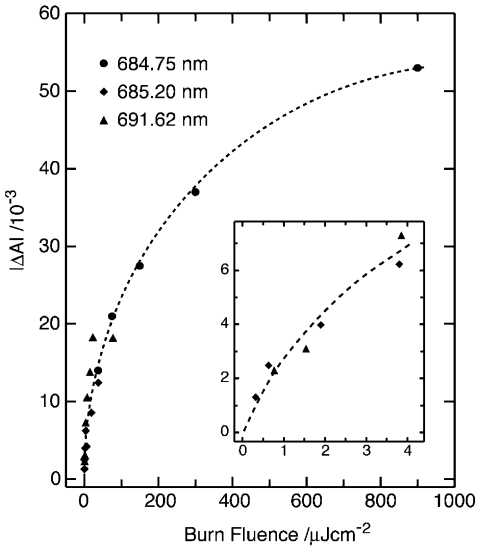

Figure 11. Hole-growth kinetics for persistent spectral holes burnt at three wavelengths in a spinach PSII core in the $S_1(Q_A^-)$ state at 2.5 K displayed as $|\Delta A|$ versus burn fluence. The dotted line is provided as a visual aid to the data. Inset shows the ultralow-fluence region, where the hole-growth kinetics approach the linear regime. The slope of the hole-growth kinetics is used to determine the hole-burning quantum efficiency.

that undergo a change following excitation. The initial hole-burning efficiency is given by[52,53]

$$\phi = \frac{N_A c(\Gamma_h) d[dA/(A_o dt)]}{[I/(h\nu)](1 - 10^{A_o})}$$

where N_A is Avogadro's number, $c(\Gamma_h)$ the effective concentration of absorbing centers that are excited by the laser (given in units of mol/cm^3), d the optical path length (given in centimeters), I the laser irradiance (given in units of W/cm^2), h Planck's constant, ν the laser frequency (in Hertz), A_o the pre-burn absorption at ν, and dA/dt the slope of the $|\Delta A|$ versus burn-time kinetic curve. In Figure 11, we have plotted $|\Delta A|$ versus burn fluence, which is proportional to the burn time.

The initial hole-burning efficiency is determined by dA/dt at $t = 0$. When the burn fluence is reduced to a range in which the hole-growth kinetics are linear, the value of dA/dt is given by the slope and no assumption about the overall functionality of the growth kinetics needs to be made. For the lowest burn fluences (<1.2 mJ/cm^2), the hole-growth kinetics are approximately linear (see inset in Figure 11). A *lower* limit for the initial hole-burning quantum efficiency can be made from these data. Independent data sets measured on individual samples with laser irradiances of ~7500 and ~60 nW/cm^2 were determined. The hole-growth curves were observed to be independent of irradiance in this range.

The hole-burning experiments performed at 685.20 nm on spinach PSII core complexes probe the absorption feature at 683.5 nm with a full width at half maximum (fwhm) of ~50 cm^{-1}. The pre-burn absorption at $\lambda = 685.20$ nm of the samples used was typically $A_o \approx 0.38$. Using the effective line width of 2.0 GHz determined in the previous section, we calculate the effective concentration of *absorbing* PSII centers to be $\sim 2.0/(30 \times 50) = 1.33 \times 10^{-3}$ of the total PSII concentration. The PSII concentration was 2.90×10^{-9} mol/cm^3 in this work. This gives the effective concentration of excited chromophores within one homogeneous line width to be 3.86×10^{-12} mol/cm^3 of PSII cores.

From the data in Figure 11, the initial hole-burning efficiency in the $S_1(Q_A^-)$ state is estimated to be $\sim 2 \times 10^{-3}$. The hole-burning kinetics exhibit a strongly dispersive behavior, with the rate of hole-burning decreasing significantly for longer burn times. Measurements of hole-growth kinetics on PSII in the $S_1(Q_A)$ state are complicated by the creation of PSII particles in the sample, which are in the $S_1(Q_A^-)$ state. Such experiments were not pursued in this work. However, from the relative hole areas in Figure 9 and corresponding hole-burning data obtained via broadband laser excitation, hole-burning in this state is 5−10 times more efficient than that for PSII in the $S_1(Q_A^-)$ state and approaches a value of 10^{-2}.

4. Discussion

Hole-burning and hole-burning action spectra have been reported for D1/D2/cytb_{559} reaction-center preparations[36,45] and for isolated CP43[43] and isolated CP47[44] proteins prepared from spinach. Each of these core fragments exhibit persistent spectral hole-burning with SDFs near 684 nm. However, there are clear differences in the fundamental characteristics of the hole-burning processes presented in this work, compared to those reported for CP43, CP47, and D1/D2/cytb_{559} fragments.

4.1. Hole-Burning Efficiencies. PSII core complexes exhibit hole-burning efficiencies that are orders of magnitude higher than those observed in core fragments. Consequently, much-higher laser fluences (typically >100 mJ/cm^2[2,20,43−45]) are required in hole-burning experiments on the isolated fragments. The hole-burning efficiency observed for spinach PSII cores in the $S_1(Q_A)$ state approaches 10^{-2} and, thus, is comparable to the efficiency of $S_1(Q_A^-)$ formation.[14] This exceptional hole-burning efficiency is present in a system exhibiting lifetimes as short as 40 ps. We have associated this remarkably high efficiency with the primary charge separation of P680*. Burn efficiencies are observed to be up to an order of magnitude lower for PSII in the $S_1(Q_A^-)$ state. This indicates that the primary charge separation in PSII is less efficient in this state. It has been suggested that, in the presence of the negatively charged Q_A^- anion, the charge separation of P680* is inhibited. The formation of $Pheo_{D1}^-$ is significantly less energetically favorable in this situation.[25]

4.2. Hole Structure: Sideholes and Photoproducts. Broadband hole-burning spectra in PSII cores are very distinct to those observed in the isolated core fragments CP43, CP47, and D1/D2/cytb_{559}. In these latter systems, hole-burning results in broad sideholes. The frequencies of the sideholes are relatively independent of the burn frequency. No such sidehole features are present in active PSII cores, and no hole-burning is observed with excitation above 676 nm. This wavelength is close to the center of the PSII core $Q_y(0,0)$ absorption envelope. Laser excitation of isolated core fragments results in resonant hole-burning for burn frequencies that extend over most of the absorption envelope.

The photoproduct associated with hole-burning in PSII cores is also very distinctive in that it is distributed across the entire SDF and not characteristically shifted to higher energies. A blue-shifted photoproduct is evident in isolated CP43[20,43] and is typical of many other systems that display nonphotochemical hole-burning.[60]

The intensity of phonon sideband holes (PSBHs) observed in PSII cores with excitation near 684 nm is very weak compared to that reported for CP43,[20,43] CP47,[44] and D1/D2/cytb_{559},[45] in which PSBHs are observable. PSBHs build to the blue side of the resonant zero-phonon hole (ZPH), whereas psuedo-PSBHs build to the red side of the ZPH (see, for

example, ref 48). The electron−phonon coupling of isolated core fragments is weak, with Huang−Rhys factors of $S \approx 0.25$ for isolated CP43,[20] $S \approx 0.2$ for the 690 nm state of isolated CP47,[44] and $S \approx 0.6-1.1$ for D1/D2/cytb_{559}.[45] In the short-burn time limit, e^{-2S} is a reasonable approximation to the ratio of the integrated intensity of the ZPH to that for the (ZPH + pseudo-PSBH).[35,48] The data in Figure 7 then clearly show that the Huang−Rhys factor (S) for the ∼684-nm SDF in PSII core complexes is remarkably small.

4.3. Excited-State Lifetimes. The decay of the excited state, and many alternative processes, can broaden spectral holes. Consequently, excited-state lifetimes as determined by hole-widths in hole-burning spectroscopy provide a *lower* limit to their actual value. By comparison, pump−probe methods may *overestimate* excited-state lifetimes, because of technical limitations in fast response systems. Persistent spectral hole-burning favors the observation of long-lived excited states as holewidths become narrow and far easier to detect and characterize.

At low temperatures (<10 K), PSII cores do not emit strongly out of narrow band state(s) near 683.5 nm.[19,61] The dominant emission of PSII cores is broad, peaking near 695 nm. This broad emission can be attributed to a chl *a* in CP47.[19,61] This assignment is supported by the observation that low-temperature emission spectra of PSII cores and isolated CP47 in this spectral region are both similar to that of D1/D2/cytb_{559}/CP47 particles. PSII cores emit with a similar quantum efficiency as isolated CP47.[57,61]

Isolated CP43 particles emit in a relatively narrow region near 683 nm at low temperatures, and also with good quantum efficiency (∼10%). Several experiments have indicated that emission has been identified as originating from two states (labeled A and B), both absorbing in a narrow but composite band near 682 nm.[43,62] Hole-burning experiments established a radiative lifetime-limited holewidth of ∼40 MHz in the A state.[43]

Low-fluence, narrow-band hole-burning has been observed in D1/D2/cytb_{559} preparations,[15,36] also providing line widths for hole-burning near 682 nm that correspond to radiative lifetimes of chl *a* (∼8 ns). The action spectrum extends over a very broad range, from 660 nm to 690 nm.

Our hole-burning experiments establish the existence of a composite SDF in both spinach BBYs and PSII cores as well as in *syn*. 6803 PSII cores. All SDFs have a narrow peak near 684 nm. The lifetime of the excited-state in this region in spinach cores in the $S_1(Q_A^-)$ and the $S_1(Q_A)$ states were determined to be ≥160 and ≥40 ps, respectively. We have suggested that CP43 is *not* responsible for the entire absorption peak at 683.5 nm in spinach cores, and that P680 absorbs strongly in this region.[17] Having determined homogeneous holewidths from measurements, it seems unlikely that the hole-burning observed in this work can be attributed to direct excitation of—and, thus, subsequent hole-burning in—P680*. If this were to occur, it would constrain the lifetime of P680* to be ≥40 ps, which is more than 10 times longer than the generally accepted value at low temperature (see Introduction). As mentioned in the Introduction, photon echo experiments[32] have been modelled to show strongly dispersive charge-separation kinetics. The range of rates was from $(1.5\ \text{ps})^{-1}$ to $\sim(1\ \text{ns})^{-1}$) in D1/D2/cytb_{559} preparations at 1.3 K. The hole-burning observed in our samples cannot be easily attributed to burning of the lowest-energy reaction center transition of a small fraction of PSII centers having long charge-separation times. First, deep spectral holes remain narrow, and, thus, a *majority* of the reaction centers would need to have charge-separation lifetimes of >40 ps. Second, the SDF (see Figure 8) shows that two electronic states contribute to hole-burning. Higher-lying excitonic components of the reaction center would relax within <1 ps and, thus, would not result in narrow spectral holes.

We propose that the state(s) in CP43 that cause fluorescence in the isolated protein transfer excitation to P680 in ≥40 ps in the intact core and the subsequent hole-burning in PSII is attributed to a mechanism that involves charge separation in P680*. The rate of excitation transfer from the CP43 fluorescent states to P680 when PSII is in the (Q_A^-) state would be ≥160 ps.

Our holewidth measurements suggest a CP43 state in intact PSII cores that has a lifetime of <160 ps. Thus, radiative emission from such a "slow transfer" state in CP43 would be weak (≥160 ps/∼8 ns, or <2% quantum efficiency). This is consistent with PSII core emission spectra that show only weak emission in the 683 nm region. The spectral position of the CP43 slow transfer states in *syn*. 6803, as inferred from hole-burning action spectra, is located at slightly higher energy than that in spinach. We have reported[14,17] that the strong negative low-temperature CD feature observed in spinach PSII cores at 683.5 nm is split in *syn*. 6803 into two features, at 681.1 and 683.8 nm. We had tentatively assigned the lower-energy feature to P680 and the higher-energy feature to CP43. On current evidence, this assignment would be inverted, with the lower-energy component being associated with the slow transfer state in CP43 in *syn*. 6803.

4.4. The Lowest-Energy Excited State of P680. Our absorption and hole-burning experiments are performed within the temperature range of 1.7−10 K and with irradiances as low as 10 nW/cm^2. Sample heating, particularly at the lowest irradiances used, is negligible. Implicit in an assignment of slow transfer states in CP43 that results in hole-burning induced by charge separation in intact PSII, is the presence of an excited state of P680 at an accessible energy. At 1.7 K, the thermal Boltzmann energy (kT) is only 1.2 cm^{-1}. Thermal activation beyond $5kT$ (6 cm^{-1} at 1.7 K) becomes increasingly unlikely. We are forced to conclude that P680 must absorb at wavelengths of >684 nm in both spinach and *syn*. 6803. The requirement that the lowest excited state of P680 be at a lower energy than 14 620 cm^{-1} (684 nm) is enforced by our observation of complete and efficient Q_A^- formation.

We propose that a broad absorption of P680 extends to lower energy and underlies the CP47 absorption in this region. This proposal can account for the very high efficiency and deep (50%) hole-burning achievable in the 690 nm trap chl *a* of CP47 in PSII cores when P680 absorption in this region is relatively weak. The dominant absorption in the 685−695 nm region of PSII cores remains the slow transfer state in CP47. From hole-burning experiments, the lifetime of this state is ∼600 ps for PSII in the $S_1(Q_A^-)$ state and is ∼4 times longer than that of the corresponding CP43 slow transfer state. A longer lifetime of the CP47 slow transfer state is consistent with a ∼9% emission quantum efficiency of PSII cores at 4 K[61] (660 ps/8 ns = 8%). We propose that significant excitation transfer from the CP47 slow transfer state occurs to the lowest-energy state of P680.

These arguments allow for the possibility of efficient excitation transfer from both CP43 and CP47 slow transfer states to P680 with high efficiency (up to 90%). P680 excitation results in both efficient Q_A^- formation when a PSII sample prepared in the $S_1(Q_A)$ state is excited and efficient hole-burning for samples in either the $S_1(Q_A^-)$ or $S_1(Q_A)$ states. The emission efficiency of PSII cores at room temperature is known to be ∼3 times lower when Q_A is reduced (the closed state) than when

Q_A is oxidized (the open state). Unless low-temperature emission experiments are made at extraordinarily low fluence (<5 mJ/cm^2), spectra will invariably be recorded for the equivalent of samples prepared in the closed $S_1(Q_A^-)$ state.[25] Emission excitation illumination will rapidly photoconvert an $S_1(Q_A)$ sample to the $S1(Q_A^-)$ state.

The lowest-energy excited state of bacterial reaction centers is known to be significantly broader than higher states (see, for example, Mar[63]). Therefore, a correspondingly broad lowest-energy excitation of a primary donor chromophore is not without precedent. The origin of this broadening has been the subject of ongoing discussion.[64−66] The energy spacing between the narrow higher-energy P680 band near 684 nm and a putative broader band near 690 nm is ∼130 cm^{-1} and, thus, is well within the range suggested by dipole−dipole couplings between closest interpigment distances of the D1/D2 chl *a* and pheo *a* molecules.[3−5,7,67]

Our analysis of band areas in PSII cores[1] suggested that the low-energy tail was reasonably well accounted for by one (CP47) chl *a*. We further estimate that any underlying absorption is likely to have an area corresponding to <0.2 chl *a*. This indicates that a dominant P680 coupling may be present between parallel transition dipoles. This arrangement would result in a weak lowest Davydov (exciton) component, as is observed in some dye aggregates.[68] Such an arrangement is different from the situation in the special pair in bacterial reaction centers, where the strongest coupling is between bacteriochlorophylls with approximately antiparallel transition dipoles. X-ray data[3−5] establish that the Q_y transition dipoles of P_{D1} and P_{D2} are also approximately antiparallel. However, transition dipoles of P_{D1}/Chl_{D2} and P_{D2}/Chl_{D1} pairs are close to parallel, and their molecular separation is only slightly greater than that of P_{D1}/P_{D2}. An assignment of a weak lowest-energy exciton component of P680 calls for a detailed investigation and further consideration.

4.5. Hole-Burning Mechanism. A widely applied model for nonphotochemical hole-burning[60] describes the chromophore potential-energy surface as a two-level system (TLS). Hole-burning results from tunneling between excited-state TLSs, and, consequently, the efficiency of hole-burning is related to the excited-state lifetime. As mentioned previously, the lifetime of our hole-burning states are much shorter than the fluorescence lifetime of chl *a*; therefore, conventional nonphotochemical hole-burning can be expected to be correspondingly less efficient. Because efficiencies of fluorescent pigments are typically only $10^{-3}-10^{-}$,[6] an alternate hole-burning mechanism is required.

We propose that when P680* charge separates, following excitation from a slow transfer pigment in CP43 or CP47, subtle changes in protein−pigment conformations occur. These changes may result from structural reorganizations of the protein and the transition energy of intercalated pigments may then be subtly altered. The transition energies of those chromophores directly excited via laser excitation will shift to slightly different values. The transition energies of chromophores not directly excited are not likely to be strongly correlated. The result is a spectral hole at the laser frequency with no sidehole features associated with other pigments. Significantly, the hole-burning efficiency now is *not* dependent on the lifetime of the slow transfer state, but rather on the probability that P680 excitation and charge separation ensues. We do not observe a large change in hole-burning efficiency between the 160-ps CP43 state and the 600-ps CP47 state for PSII cores in the $S_1(Q_A^-)$ state. This supports a hole-burning mechanism that is independent of excited-state lifetime.

A "charge transfer" hole-burning mechanism is not without precedent. A similar mechanism, which involves charge separation between pairs of interacting metallophthalocyanines, has been suggested to explain the hole-burning observed for these chromophores trapped in frozen rare-gas matrixes.[69,70]

4.6. P680 Charge-Separation Rate. Our observation of long-lived states in PSII cores, transferring excitation to P680 at low temperatures, does not provide support for the "shallow trap" model of P680. In this model, excitation equilibration between P680 and all antenna pigments is considered to be faster than the charge separation rate of P680. However, at physiological temperatures, the slow transfer states may be bypassed by thermally activated excitation transfer processes and, thus, may not be rate-limiting.

The absence of hole-burning at wavelengths of <676 nm in active PSII, along with the absence of emission at these wavelengths, is consistent with the belief that excitation transfer from pigments absorbing at these higher energies is indeed faster than ∼500 fs. The potential exists that *direct* low-temperature excitation of the lowest-energy excited state of P680 may result in hole-burning in this absorption, particularly for a PSII sample in the $S_1(Q_A)$ configuration. The holewidth here may provide the first *direct* measure of the rate of charge separation in *native* P680*. Such holes may be 30−300 GHz wide, corresponding to a charge-separation rate of 1−10 ps. They could be expected to be relatively shallow if the absorption of the lowest excited state of P680 is, indeed, weak. Such a hole would be observed in parallel with the sharp (0.5 GHz) CP47 holes reported here. We note that, in the bacterial reaction center, narrow-band excitation into the lowest-energy primary donor band leads to extremely broad spectral holes whose width does not relate to the charge-separation rate.

5. Conclusions

We have identified highly efficient persistent spectral hole-burning in the active photosystem II (PSII), which we associate with a charge-separation mechanism that involves native P680*. Lifetime-limited holewidths that have been determined to be in the 0.5−2.0 GHz range indicate the presence of long-lived excited-states in CP43 and CP47, which transfer excitation to P680 with good efficiency. The ensuing charge-separation process is held responsible for the high hole-burning efficiency observed.

Efficient hole-burning and electrochromic shifts associated with Q_A^- formation occur upon low-fluence excitation in the 685−695 nm spectral range. This is interpreted by proposing a weak, broad lowest excited state of P680 underlying the broad CP47 absorption in this range. At low temperatures, excitation of the "trap" CP47 in intact PSII leads to efficient charge separation. The "slow transfer" states in CP43 and CP47 may, indeed, serve a significant function in *active* PSII if these processes are rate-limiting at physiological temperatures.

References and Notes

(1) Smith, P. J.; Peterson, S.; Masters, V. M.; Wydrzynski, T.; Styring, S.; Krausz, E.; Pace, R. J. *Biochemistry* **2002**, *41*, 1981.

(2) Blankenship, R. E. *Molecular Mechanisms of Photosynthesis*; Blackwell Science Ltd.: Oxford, 2002.

(3) Ferreira, K. N.; Iverson, T. M.; Maghlaoui, K.; Barber, J.; Iwata, S. *Science* **2004**, *303*, 1831.

(4) Zouni, A.; Witt, H. T.; Kern, J.; Fromme, P.; Kraub, N.; Saenger, W.; Orth, P. *Nature* **2001**, *409*, 739.

(5) Kamiya, N.; Shen, J.-R. *Proc. Natl. Acad. Sci. U.S.A.* **2003**, *100*, 98.

(6) Jankowiak, R.; Hayes, J. M.; Small, G. J. *J. Phys. Chem. B* **2002**, *106*, 8803.

(7) Dekker, J. P.; van Grondelle, R. *Photosynth. Res.* **2000**, *63*, 195.
(8) Mino, H.; Kawamori, A. *Biochim. Biophys. Acta* **2001**, *1503*, 112.
(9) Peloquin, J. M.; Britt, R. D. *Biochim. Biophys. Acta* **2001**, *1503*, 96.
(10) Kuzek, D.; Pace, R. J. *Biochim. Biophys. Acta* **2001**, *1503*, 123.
(11) Geijer, P.; Peterson, S.; Åhrling, K. A.; Deák, Z.; Styring, S. *Biochim. Biophys. Acta* **2001**, *1503*, 83.
(12) Hanley, J.; Deligiannakis, Y.; Pascal, A.; Faller, P.; Rutherford, A. W. *Biochemistry* **1999**, *38*, 8189.
(13) Faller, P.; Pascal, A.; Rutherford, A. W. *Biochemistry* **2001**, *40*, 6431.
(14) Peterson Årsköld, S.; Masters, V. M.; Prince, B. J.; Smith, P. J.; Pace, R. J.; Krausz, E. *J. Am. Chem. Soc.* **2003**, *125*, 13063.
(15) Groot, M. L.; Dekker, J. P.; van Grondelle, R.; den Hartog, F. T. H.; Völker, S. *J. Phys. Chem.* **1996**, *100*, 11488.
(16) Greenfield, S. R.; Seibert, M.; Wasielewski, M. R. *J. Phys. Chem. B* **1999**, *103*, 8364.
(17) Peterson Årsköld, S.; Prince, B. J.; Krausz, E.; Smith, P. J.; Pace, R. J.; Picorel, R.; Seibert, M. *J. Lumin.* **2004**, *108*, 97.
(18) Prince, B. J.; Krausz, E.; Peterson Årsköld, S.; Smith, P. J.; Pace, R. J. *J. Lumin.* **2004**, *108*, 101.
(19) Masters, V.; Smith, P.; Krausz, E.; Pace, R. *J. Lumin.* **2001**, *94*, 267.
(20) Hughes, J. L.; Prince, B. J.; Peterson Årsköld, S.; Krausz, E.; Pace, R. J.; Picorel, R.; Seibert, M. *J. Lumin.* **2004**, *108*, 131.
(21) Svensson, B.; Etchebest, C.; Tuffery, P.; van Kan, P.; Smith, J.; Styring, S. *Biochemistry* **1996**, *35*, 14486.
(22) Greenfield, S. R.; Wasielewski, M. R. *Photosynth. Res.* **1996**, *48*, 83.
(23) Durrant, J. R.; Hastings, G.; Joseph, D. M.; Barber, J.; Porter, G.; Klug, D. R. *Proc. Natl. Acad. Sci. U.S.A.* **1992**, *89*, 11632.
(24) Yoder, L. M.; Cole, A. G.; Sension, R. J. *Photosynth. Res.* **2002**, *72*, 147.
(25) Schatz, G. H.; Brock, H.; Holzwarth, A. R. *Proc. Natl. Acad. Sci. U.S.A.* **1987**, *84*, 8414.
(26) Schatz, G. H.; Brock, H.; Holzwarth, A. R. *Biophys. J.* **1988**, *54*, 397.
(27) Schelvis, J. P. M.; Germano, M.; Aartsma, T. J.; van Gorkom, H. J. *Biochim. Biophys. Acta* **1995**, *1230*, 165.
(28) de Weerd, F. L.; van Stokkum, I. H. M.; van Amerongen, H.; Dekker, J. P.; van Grondelle, R. *Biophys. J.* **2002**, *82*, 1586.
(29) Müller, M. G.; Hucke, M.; Reus, M.; Holzwarth, A. R. *J. Phys. Chem.* **1996**, *100*, 9537.
(30) Greenfield, S. R.; Seibert, M.; Govindjee; Wasielewski, M. R. *Chem. Phys.* **1996**, *210*, 279.
(31) Donovan, B.; Walker, L. A., II; Yocum, C. F.; Sension, R. J. *J. Phys. Chem.* **1996**, *100*, 1945.
(32) Prokhorenko, V. I.; Holtzwarth, A. R. *J. Phys. Chem. B* **2000**, *104*, 11563.
(33) Germano, M.; Gradinaru, C. C.; Shkuropatov, A. Y.; van Stokkum, I. H. M.; Shuvalov, V. A.; Dekker: J. P.; van Grondelle, R.; van Gorkom, H. J. *Biophys. J.* **2004**, *86*, 1664.
(34) Jankowiak, R.; Hayes, J. M.; Small, G. J. *Chem. Rev.* **1993**, *93*, 1471.
(35) Reddy, N. R. S.; Lyle, P. A.; Small, G. J. *Photosynth. Res.* **1992**, *31*, 167.
(36) den Hartog, F. T. H.; Vacha, F.; Lock, A. J.; Barber, J.; Dekker, J. P.; Völker, S. *J. Phys. Chem. B* **1998**, *102*, 9174.
(37) Reddy, N. R. S.; Kolaczkowski, S. V.; Small, G. J. *Science (Washington, DC)* **1993**, *260*, 68.
(38) Jankowiak, R.; Rätsep, M.; Hayes, J.; Zazubovich, V.; Picorel, R.; Seibert, M.; Small, G. J. *J. Phys. Chem. B* **2003**, *107*, 2068.
(39) Hala, J.; Vacha, M.; Dian, J.; Ambroz, M.; Adamec, F.; Prasil, O.; Komenda, J.; Nedbal, L.; Vacha, F.; Mares, J. *J. Lumin.* **1991**, *48&49*, 295.
(40) Stranger, R.; Dubicki, L.; Krausz, E. *Inorg. Chem.* **1996**, *35*, 4218.
(41) Lewis, M. L.; Riesen, H. *J. Phys. Chem. A* **2002**, *106*, 8039.
(42) Hughes, J. L.; Riesen, H. *J. Phys. Chem. A* **2003**, *107*, 35.
(43) Jankowiak, R.; Zazubovich, V.; Rätsep, M.; Matsuzaki, S.; Alfonso, M.; Picorel, R.; Seibert, M.; Small, G. J. *J. Phys. Chem. B* **2000**, *104*, 11805.
(44) Chang, H. C.; Jankowiak, R.; Yocum, C. F.; Picorel, R.; Alfonso, M.; Seibert, M.; Small, G. J. *J. Phys. Chem.* **1994**, *98*, 7717.
(45) Jankowiak, R.; Rätsep, M.; Picorel, R.; Seibert, M.; Small, G. J. *J. Phys. Chem. B* **1999**, *103*, 9759.
(46) Tang, D.; Jankowiak, R.; Seibert, M.; Yocum, C. F.; Small, G. J. *J. Phys. Chem.* **1990**, *94*, 6519.
(47) Avarmaa, R. A.; Rebane, K. K. *Spectrochim. Acta, Part A* **1985**, *41A*, 1365.
(48) Johnson, S. G.; Lee, I.-J.; Small, G. J. Solid State Spectral Line-Narrowing Spectroscopies. In *Chlorophylls*; Scheer, H., Ed.; CRC Press: Boca Raton, FL, 1991; p 739.
(49) Reddy, N. R. S.; Picorel, R.; Small, G. J. *J. Phys. Chem.* **1992**, *96*, 6458.
(50) Völker, S. Spectral Hole-Burning in Crystalline and Amorphous Organic Solids. Optical Relaxation Processes at Low Temperature. In *Relaxation Processes in Molecular Excited States*; Fünfschilling, J., Ed.; Kluwer Academic Publishers: Dordrecht, Boston, London, 1989; p 113.
(51) Moerner, W. E., Ed. *Persistent Spectral Hole-Burning: Science and Applications*; Springer−Verlag: Berlin, Heidelberg, 1988; Vol. 44, p 315.
(52) Riesen, H. *Chem. Phys. Lett.* **2004**, *383*, 512.
(53) Riesen, H.; Hughes, J. L. *Chem. Phys. Lett.* **2003**, *372*, 563.
(54) Kenney, M. J.; Jankowiak, R.; Small, G. J. *Chem. Phys.* **1990**, *146*, 47.
(55) Kim, W.-H.; Reinot, T.; Hayes, J. M.; Small, G. J. *J. Phys. Chem.* **1995**, *99*, 7300.
(56) Rätsep, M.; Blankenship, R. E.; Small, G. J. *J. Phys. Chem. B* **1999**, *103*, 5736.
(57) Groot, M.-L.; Peterman, E. J. G.; van Stokkum, I. H. M.; Dekker, J. P.; van Grondelle, R. *Biophys. J.* **1995**, *68*, 281.
(58) den Hartog, F. T. H.; Dekker, J. P.; van Grondelle, R.; Völker, S. *J. Phys. Chem. B* **1998**, *102*, 11007.
(59) Boxer, S. G.; Gottfried, D. S.; Lockhart, D. J.; Middendorf, T. R. *J. Chem. Phys.* **1987**, *86*, 2439.
(60) Shu, L.; Small, G. J. *Chem. Phys.* **1990**, *141*, 447.
(61) Dekker, J. P.; Hassoldt, A.; Pettersson, Å.; van Roon, H.; Groot, M.-L.; van Grondelle, R. On the Nature of the F695 and F685 Emission of Photosystem II. In *Photosynthesis: From Light to Bioshpere*; Mathis, P., Ed.; Kluwer Academic Publishers: Dordrecht, Boston, London, 1995; Vol. 1; p 53.
(62) Groot, M.-L.; Frese, R. N.; de Weerd, F. L.; Bromek, K.; Pettersson, A. *Biophys. J.* **1999**, *77*, 3328.
(63) Mar, T.; Gingras, G. *Biochemistry* **1995**, *34*, 9071.
(64) Moore, L. J.; Zhou, H.; Boxer, S. G. *Biochemistry* **1999**, *38*, 11949.
(65) Zhou, H.; Boxer, S. G. *J. Phys. Chem. B* **1997**, *101*, 5759.
(66) Small, G. J. *Chem. Phys.* **1995**, *197*, 239.
(67) Durrant, J. R.; Klug, D. R.; Kwa, S. L. S.; von Grondelle, R.; Porter, G.; Dekker, J. P. *Proc. Natl. Acad. Sci., U.S.A.* **1995**, *92*, 4798.
(68) Craig, D. P.; Walmsley, S. H. *Excitons in Molecular Crystals*; W. A. Benjamin, Inc.: New York, Amsterdam, 1968.
(69) Prince, B. J.; Williamson, B. E.; Reeves, R. J. *J. Lumin.* **2001**, *93*, 293.
(70) Dunford, C. L.; Williamson, B. E.; Schatz, P. N.; Gasyna, Z.; Krausz, E.; Riesen, H. *Chem. Phys. Lett.* **1996**, *260*, 522.